Use of Karl Fischer titration for the localized measurement of water content in FRP composite aircraft parts removed from service

Camille Gillet, Wilfried Splawski, Florian Aguirre, Bouchra Hassoune-Rhabbour, Tatiana Tchalla, Valérie Nassiet

Journal of Composite Materials
XX(X):1–13

DOI: 10.1177/ToBeAssigned
www.sagepub.com/
SAGE

Use of Karl Fischer titration for the localized measurement of water content in FRP composite aircraft parts removed from service

Camille Gillet[12], Wilfried Splawski[2], Florian Aguirre[1], Bouchra Hassoune-Rhabbour[1], Tatiana Tchalla[2], Valérie Nassiet[1]

Abstract

Moisture content measurements are performed on scrapped Outlet Guide Vanes that have operated in different climates. These measurements are made by three Karl Fischer titration methods. The results are separated into two parts. On one side, a comparison of these different techniques highlights their advantages and disadvantages. The methods for studying the samples and the duration of the tests differ. The standard method is not sufficient to extract all the water from the samples. The chemical extraction and grinding methods provide higher water content. On the other side, a mapping of the water content through three scrapped OGV blades is performed with the Karl Fischer titration. Differences are observed according to the service area climate. Concentration gradients are also visible within the part, with more water at the leading edges and less water in the foam. Parts that have flown in hot and humid regions have the lowest water contents by standard Karl Fischer titration. These measurements are compared with the analysis of the damage they have been subjected to. They allow to highlight the composite material degradation, manifested by resin erosion, which is more significant for parts that have operated in wet and humid areas. This erosion involves a lower resin percentage and could explain the lower water contents measured.

Keywords

Composite material, Outlet Guide Vane, Flight service, Environmental effects, Hygrothermal ageing, water content, Karl Fischer titration

Introduction

For more than fifty years, fibre-reinforced polymer (FRP) composite materials have proven their importance in aeronautics because their excellent properties allow a considerable gain in the mass of structures. The current ecological revolution is imposing on the aeronautics industry to reconsider its fundamental concepts to reduce the environmental footprint of air transport drastically. Aircraft manufacturers have therefore started to reduce the non-useful on-board weight to impact aircraft fuel consumption positively and thus reduce the environmental damage associated with fossil fuel consumption. This objective involves replacing more metal parts with organic matrix composite materials. While they were mainly used on secondary parts, they are now used on primary structural parts not exposed to high temperatures, such as the aircraft floor panels, spoilers, wings, engine fans, engine nacelles, outlet guide vanes, etc. The fuselages of the Boeing 787 and Airbus A350, or the nacelle of the Airbus A380, made of FRP composite materials, are examples of these technological advances. These developments towards composites can also be seen in aircraft engines, with acoustic panels and outlet guide vanes of the CFM 56 engine, fan cases and fan blades of the CFM LEAP or GE90 engines, etc (1).

During their service life, the polymers and composite materials used in aircraft engine parts are subjected to a complex ”natural” ageing, which has various causes. ”Normal” ageing is related to the functioning of the aircraft, such as the action of thermal peaks and continuous high-speed air flows, and to the effect of environmental stresses, such as humidity and temperature. ”Occasional” ageing can also occur, such as storms, lightning strikes, air pollution and maintenance fluids (cleaning fluid, de-icing fluid). Finally, ”exceptional” or ”abnormal” events, such as the leakage of aeronautical fluids (engine oil, hydraulic fluid, fuel). Alterations to composite material aircraft engine parts have been little studied in the literature. Nevertheless, the evolution of some composite aircraft and helicopter fuselage parts (horizontal or vertical stabilisers, ailerons, spoilers, fairings, elevators etc.) has already been examined. These materials are highly sensitive to climatic conditions which cause the degradation of macromolecular chains and interfaces under the action of temperature, humidity, solar radiation, rain, hail and snow, clouds, lightning strikes, sandstorms, dust and pollution, high speed air flows,

[1]Laboratoire Génie de Production, École Nationale d’Ingénieurs de Tarbes, Toulouse INP, Université de Toulouse, France.
[2]Safran Aircraft Engines, Villaroche site, France.

Corresponding author:
Valérie Nassiet, Laboratoire Génie de Production, INP-ENIT, Université de Toulouse, 47 Avenue d’Azereix, 65016, Tarbes, France.
Email: valerie.nassiet@enit.fr

aeronautical fluids, etc. These alterations are simultaneous and difficult to delimit. In addition, the parts are generally made of several materials and covered with coatings or paints, which contributes to the complexity of the studies. These elements all have different sensitivities to the ravages of time (2; 3; 4).

Furthermore, natural ageing is a very slow mechanism, and its effects may not be noticeable for several decades. Dexter and Baker, and Tian and Hodgkin found that after ten and twenty years of service, respectively, the aircraft and helicopter composite material fuselage parts studied showed only slight changes in their properties (5; 6). Although the take-off and flight conditions appear to be the same for all aircraft engine parts, there are notable differences depending on the service area. For example, it was found that aircraft that had flown in hot and humid areas (Gulf of Mexico, Brazil, Malaysia) showed a slight decrease in fracture toughness and slightly higher water absorption. Moisture trapped in the parts, coupled with thermal peaks experienced during take-off, intensified for supersonic flights, is the cause of the formation and propagation of micro-cracks. Water present in the matrix, at the fibre/matrix interface, in the sandwich cores or in cracks suddenly becomes trapped and damages the material by vaporising under the heat (7; 8). In hovering flight, the bound water that did not evaporate during take-off freezes in the composite micro-cracks. However, the water only turns to ice if the microcracks are large enough to allow this, in which case it becomes a glassy liquid. In this situation, there is no volume expansion and no crack propagation (9).

Nevertheless, it is essential to specify that these fuselage parts do not experience as many alterations as engine parts, as in the paper case. Indeed, any part from the engine fan is subject to thermal peaks during its service life, linked to the engine operation during take-off (about 120 °C), followed by exposure to the cold during hovering at an altitude of about 10 km (about -70 °C). These strong variations have an impact on its chemical and physical properties. Because of their function, outlet guide vanes (OGV) have to straighten the fan and are subject to stresses from laminar and turbulent flows of hot air at high pressure and the particles (dust, sand) and water droplets they carry away (10; 11; 12). Parts can also be exposed to various aeronautical fluids in the engine during normal use or by accident. Jet fuel, hydraulic fluids and de-icing fluids cause irreversible chemical modifications to metal parts (13; 14) or FRP composite parts (15; 16; 17). Pollutants in industrial areas, sulphur dioxide, oxides of nitrogen and carbon, and ozone, also have an accelerating effect on the degradation of composite materials (18). Funke and Haagen observe that SO_2 can penetrate polymer coatings and attack the part (19). Jakubowicz and Möller report that the H_2SO_4 formed with oxidised SO_2 and water can react with the $CaCO_3$ fillers of the polymers to form $CaCO_4$ (20). Pollutants can therefore modify the chemical composition of FRP composite materials. The natural ageing experienced here is, therefore a combination of different types of ageing: hygrothermal, thermo-oxidative, chemical, etc. These couplings act on each other and can accelerate the activation of chemical reactions between water, oxygen and materials. The diffusion processes are then more important. On the other hand, the couplings and their analysis require extensive experimentation. Indeed, the number of parameters and phenomena – which act on each other – is all the more important as the number of couplings increases (21; 22; 23).

Since the major differences observed are related to climatic conditions, the study focuses on the action of moisture and heat on composite material parts from aircraft engines. The consequences of moisture absorption are well known: absorption of solvents, migration of additives, plasticisation, hydrolysis, oxidation, differential swelling, depolymerisation, embrittlement, cracking, etc (24; 25; 26; 27; 28; 29). These degradations can lead to drops in glass transition temperature T_g and mechanical properties (30; 31; 32; 33). For this reason, the paper focuses on measuring the moisture percentage contained in scrapped aircraft engine parts in a global or localised approach to relate them to the degradation they have experienced.

Moisture absorption or desorption gravimetric measurements are widely used to quantify the moisture percentage in polymer or FRP composite parts. However, in the case of irreversible degradation, these gravimetric measurements can be inaccurate. In some cases, gravimetric curves reveal these degradations, which are expressed by significant mass losses (34; 35; 36; 37). In other cases, mass losses are not visible on the absorption curves but can be observed by desorption. The mass change $M(t)$ does not return to its initial value. Mass losses, therefore, occur during the absorption phase while the mass gain curve continues to increase slowly. The study of the desorption kinetics is then important to verify the presence of hidden mass losses or to highlight a chemical evolution (38; 39; 40; 41; 42; 43; 44). Numerical damage models allow to predict the mass intake or loss during the water absorption (45; 46; 47; 48).

However, temperature desorption may not be sufficient to remove bound water molecules. Zhou and Lucas report that, depending on the temperatures experienced and the ageing time, the bond strength of the water molecules to the macromolecules can increase. They show that a theoretical temperature of 140 °C is required to remove water molecules and fully desorb their epoxy resins (49). On the other hand, this prolonged exposure to heat could cause degradation by ageing and, therefore, additional mass losses. For polymers with low T_g, the high temperatures of accelerated hygrothermal ageing or thermal desorption can cause their degradation, forming and releasing volatile compounds. The measured uptake or loss in mass then no longer corresponds to the absorbed water percentage.

Other methods have been developed to measure this moisture percentage. Some authors have worked on the use of fibre optic sensors inserted into the sample during its manufacture to monitor its water uptake in situ (50; 51; 52). Other authors have applied THz spectroscopy for the detection, localisation and size measurement of water clusters in a composite material (53). Dynamic Vapour Sorption has also been studied to measure the water diffusion coefficient of a sample (39). Some water content monitoring methods are implemented using the Fourier transform near-infrared spectroscopy (FT-NIR) by performing regression and establishing the quantitative absorbance dependence on water content. This technique allows to measure the free and bound water fractions in the polymer network. Contrary to mid-infrared spectroscopy (FT-MIR), the resolution of

ν_{OH} region, related to water molecules, is improved, and it is possible to separate out the individual components (54; 55; 56).

Finally, Karl Ficher titration method is widely used to measure the water content down to ppm on organic compounds such as hydrocarbons, fertilisers or food (57; 58), as powder, paste, or solutions. However, it can give results with more uncertainty when the matrix contains hydrophobic compounds such as starch (59). Karl Fischer titration has already been used on polymers, coupled with other tests such as FTIR spectroscopy or TGA (60; 61; 62).

In the present paper, the damage experienced by OGV during their service life is studied and compared as a function of location by FTIR spectroscopy, T_g measurements by DSC and optical microscopy. In the following, the determination of the moisture percentage in composite aircraft engine parts scrapped from service is performed by Karl Fischer titration. First of all, three Karl Fischer titration methods are used and compared to measure water content after optimising its operating parameters according to the composite OGV properties. Finally, water content measurements are carried out through the OGV blades to determine whether concentration gradients are present.

Material and methods

Material

The parts studied in this paper are outlet guide vanes (OGV) from aircraft engines. These parts consist of two NACA profile blades of FRP connected to two polymer platforms. (Figure 1 (a)).

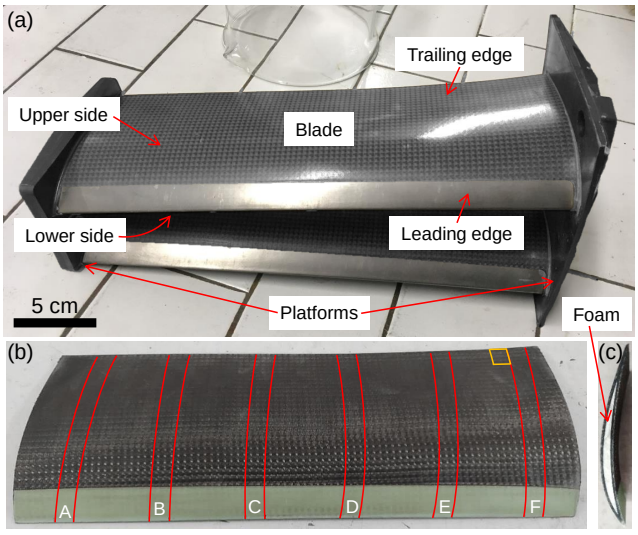

Figure 1. (a) OGV components, (b) OGV blade surface and distribution of sample cuts, (c) cross-section.

The OGV blades consist of an epoxy foam core reinforced with hollow spheres around which unidirectional plies of carbon/epoxy and carbon/glass/epoxy are draped. The leading edge is a stainless steel foil bonded with an epoxy adhesive. The stacking of the plies and the epoxy and fibre nature are confidential. In the study, only the composite parts of the blades are studied, i.e. the FRP surface on the upper and lower sides and the core foam. The foils and platforms are not investigated. The samples are cut from the blades according to the dimensions and positions given in Figure 1 (b). The yellow outlines represent the areas where the samples used for FTIR analysis, T_g measurements, and comparison of the water content measurement methods are cut. They are cut out of the trailing edge so as not to be impacted by the glue used to bond the aluminium foil to the leading edge and to avoid having a sample composed solely of composite material with no foam. The red lines, letters and numbers represent the different areas where the samples are cut to model the water content distribution in the blades.

For Karl Fischer titration analyses, the samples are cut according to their mass: 30 to 50 mg for the foam zones and 95 to 150 mg for the composite material zones.

An unaged OGV is used to compare the damage experienced by aged OGV. 4 aged OGV are studied. The measurement methods are compared using an OGV that has not experienced a flight service life and has been naturally aged on the ground in a factory in France (OGV 1). The distribution of the water content in the OGV blade according to its service life is studied using three scrapped OGV. They had a flight service life and evolved in different areas and durations: OGV 2) South East Asia, OGV 3) Middle East, OGV 4) Europe. For confidentiality reasons, their ageing time is divided by the ageing time of OGV 1 as a ratio in Table 1.

Methods

Optical microscopy The surface morphology is analysed with a Keyence VHX6000 3D optical microscope. The Z-resolution of the optical microscope is in the order of 200 nm. A $\times 1000$ objective is used. Using a scan stitching function allows obtaining a scanned area size larger than the field size imposed by the objective. Each morphological analysis is performed three times per sample to ensure repeatability.

DSC DSC analyses are performed to measure the glass transition temperature T_g of OGV samples. Samples were run in a TA Instruments DSC Q200 with an underlying heating rate of 10 °C/min with a nitrogen flow. Samples are encapsulated in aluminium pans. A sample size of between 10 and 20 mg was used. Each DSC thermogram is performed three times per sample to ensure repeatability.

Fourier transform infrared spectroscopy (FTIR) Fourier transform infrared spectroscopy is used to obtain information on the chemical bonds of functional groups on the surface of OGV samples. The bonds vibrate at a given frequency, which depends on the atoms and the environment of the bond. Measurements were performed in absorbance on the Perkin-Elmer Spectrum One apparatus with the attenuated total reflectance (ATR) module. The detector type is a mid-infrared toroidal grating spectrograph (MIR TGS) with a wavenumber range of 4000-650 cm^{-1}. Crystal is a Diamond/ZnSe. After a background, eight scans were performed with a resolution of 1 cm^{-1}. Corrections of the wavenumber thickness dependence and the baseline were made. The spectra are normalised to the 1510 cm^{-1} peak, corresponding to the aromatic C=C band elongation, unaffected by ageing (63; 64; 65). FTIR analyses were conducted as trifold determination per sample to ensure repeatability.

Table 1. OGV ageing times divided to the ageing time of OGV 1.

Type	Unaged	OGV 1	OGV 2	OGV 3	OGV 4
Ratio (year/year)	-	1	0.55	0.7	1.3

Karl Fischer titration Karl Fischer titrator analysis allows the water content determination of a sample from a raw, finished or aged product. It is based on an oxidation reaction of sulphur dioxide by iodine in a methanol hydroxide solution according to the Bunsen reaction (Equation 1) (66).

$$\begin{aligned} &ROH + SO_2 + R'N \rightarrow \\ &[R'NH]SO_3R + H_2O + I_2 + 2R'N \rightarrow \\ &2[R'NH]I + [R'NH]SO_4R \end{aligned} \quad (1)$$

with ROH primary alcohol, SO_2 sulphur dioxide, $R'N$ pyridine base, $[R'NH]SO_3R$ alkyl sulphite intermediate salt, H_2O water, I_2 iodine, $[R'NH]$ hydroiodic acid salt and $[R'NH]SO_4R$ alkyl sulphate salt.

Two types of analysis are possible: volumetric or coulometric. In both cases, titration is carried out by adding iodine until an excess appears. In volumetric titration, the titrant volume is taken to determine the present water volume. For reasons of precision and considering that the water volumes are less than 1 mg, a coulometric study was chosen. It uses Faraday's law and determines the water quantity from the quantity of alternating current A and the total charge passed Q during a time t. The direct current does not allow an accurate analysis because it detects multiple parasites.

Equation 2 allows the determination of the water quantity for values between 1 ppm and 5 % of water in total Karl Fischer solution:

$$Q = A \times t \quad (2)$$

with 1 mg of water $\Leftrightarrow$ 10,72 C.

In order to respect the stoichiometry between water and iodine (2:1) and to have a correct reaction speed, it is recommended to have a pH between 5 and 7. The excess iodine detection can be visual, photometric or potentiometric. Potentiometric is the method installed on the apparatus used. It is also required to perform a "blank" to determine the water content of the laboratory atmosphere. The samples used must have a minimum mass of three times that of the blank.

A Karl Fischer titration is divided into three parts. First of all, a drift analysis is performed (conditioning) in order to respect a value of about 12 μg.min^{-1}. The drift is the quantity of iodine per unit of time that is generated in the system. The second step is the adjustment of the experimental parameters. The last step is the actual analysis of the amount of water present in the material. In order to have the same atmospheric conditions, the vials are dried at 70 °C overnight and placed in a desiccator until use. The samples are placed in the vials after being weighed. They are then sealed. During the blank or analysis, the sample is raised to a fixed temperature defined by a preliminary gradient study, detailed later in this paper. The analysis time depends on the amount of water content, and measurements are taken every 2 seconds. The test ends when the stabilisation criteria are reached. The test time is set at 300 s for a dry sample and 1200 s when it has been wet aged to avoid exceeding the threshold where fluctuations in water content due to purge gas would be noticeable. The titration solution used is changed every 19 tests. Variations to this method are also used in this paper: by chemical extraction and by grinding. The instrument used in this paper is the Karl Fischer Coulometer Titrino 831 titrator from Metrohm.

Results

Damage assessment

Optical microscopies performed on the OGV are shown in the Figure 2. On the upper side, the service-aged surfaces (OGV 2-3-4) show numerous cracks. Fibres are exposed in some areas, suggesting matrix degradation. OGV 2, which flew in South-East Asia, shows the most cracks and material loss. OGV 3, which flew in the Middle East, particularly have small impacts of a hundred micrometres. As some of their aircraft flew in desert areas, it is possible that these impacts were caused by sandstorms. On the lower side, the damage is considerably more intense than on the upper side, as the shape of the fabric is visible. Most of the fibres have been exposed by the erosion of the resin. Areas of degradation are also visible on OGV 4. OGV 1 shows few degradations; only scratches and yellowing are seen. There is no difference between the upper and lower sides. The lower side, which was initially identical to the upper side, is therefore much more damaged due to flight service life. This phenomenon could be due to abrasion of the surface with solid particles in the air circulated by the engine, or fluid friction with the air. Since the blade NACA profile is asymmetric, the air flow is not homogeneous between the upper and lower surface.

Glass transition temperature T_g measurements made on OGV FRP surfaces and foams are given in Table 2. When unaged, the FRP surface has a T_g equal to 179.5 $\pm$ 5.1 °C. It drops by about 19 °C after ground ageing (OGV 1). For parts that have experienced a service flight, it decreases by around 23.5 °C after ageing in Southeast Asia, by around 6 °C after ageing in Europe, and by around 5.7 °C after ageing in the Middle East. Thus, the T_g of FRP surfaces seems to depend more on flight location than on flight time. The foam T_g shows less variation. After ageing on the ground or in flight service, it varies by $\pm$ 5 °C around the value of T_g of the unaged OGV, equal to 135.1 $\pm$ 0.4 °C. The climatic effects seem not to have reached the core of the OGV.

The FTIR spectra performed on the FRP surfaces of the OGV are shown in Figure 3. The band at 3650-3100 cm^{-1} is related to O–H bonds. Its increase indicates the presence of water in the OGV. The part of the band at 3650-3350 cm^{-1} is associated with free water, while the part at 3350-3100 cm^{-1} corresponds to bound water. The whole band expands and intensifies with ageing, indicating the presence of water in the OGV (56). The OGV 1 band increases slightly to

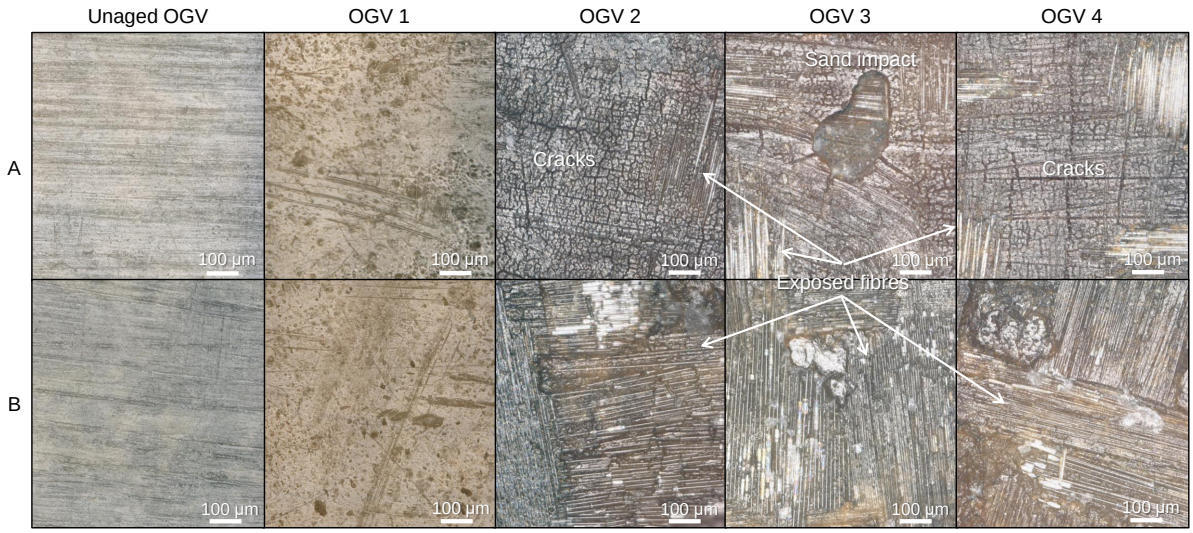

Figure 2. Optical microscopies of unaged and aged (1, 2, 3 and 4) OGV surfaces: (A) upper side, (B) lower side.

Table 2. Glass transition temperature T_g of the FRP surfaces and foams of OGV.

Type	Unaged	OGV 1	OGV 2	OGV 3	OGV 4
$T_{g\ FRP}$ (°C)	179.5 ± 5.1	160.5 ± 3.2	156.0 ± 10.4	173.8 ± 0.2	173.5 ± 0.2
$T_{g\ Foam}$ (°C)	135.1 ± 0.4	141.5 ± 3.5	137.8 ± 3.0	135.8 ± 3.8	130.4 ± 0.4

3350-3100 cm^{-1}. It remains unchanged at 3650-3350 cm^{-1}. On the contrary, an increase of the part between 3650-3350 cm^{-1} is visible for OGV 2, 3 and 4 and may correspond to the presence of free water in the rooms. The increase in this band portion is particularly sharp for OGV 2, which could be related to its damage and the presence of erosion and micro-cracks (55). The peak band at 3150-2985 cm^{-1} and 2985-2850 cm^{-1} can be associated with the C–H bonds of alkanes and the N–H bonds of first and second amines (67; 68; 69). It is reduced after the flight service. This attenuation may be related to epoxy matrix degradations, following chain scissions that may be caused by hydrolysis and oxidation. Some peaks are related to oxidation intensification, such as the peaks at 1740, 1650 and 1620 cm^{-1} of C=O bonds (31; 70). They are particularly strong for OGV 3, which flew in a warmer and drier climate. They are moderate for OGV 2 and 4. They are very low for unaged or ground-aged parts (OGV 1), probably because they were not subjected to the thermal peaks caused during the aircraft's take-off. A series of peaks also appear at 1400 and 870 cm^{-1} in OGV 2, 3 and 4, which have had a flight service life. As these peaks appear and are intense, they would not appear to be associated with matrix degradation. They could be attributed to contaminants' presence, such as pollution, dust, fluids, or chemical evolution. Jakubowicz et al. observed an increase in a peak series between 1800 and 875 cm^{-1} on the surface of their naturally aged PVC. They associate this with various causes: pollution, chemical modification of the material's fillers by pollution, and formation of HCl following the degradation of the PVC. They observed a partial reduction in these peaks by cleaning with ethanol the surfaces (20).

FTIR spectra are also performed on the OGV foams. They are shown in Figure 4. As with the surfaces, the 3650-3150 cm^{-1} band, associated with O–H bonds, increases

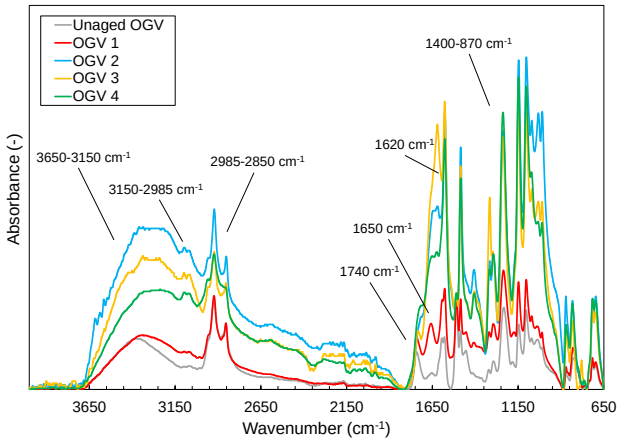

Figure 3. FTIR spectra of OGV surfaces (upper side).

when ageing is experienced. It is significant for OGV 1 and 2. For OGV 2, this is explained by the hot and humid climate in which it evolves. For OGV 1, it could be that ground ageing, without a thermal peak due to take-off, may preserve the foam from drying. For OGV 3, this band is almost as weak as for OGV unaged, suggesting that the moisture has not penetrated the core foam significantly. The bands at 3125-3025 and 3025-2825 cm^{-1}, related to the C–H and N–H bonds, decrease following the ageing as previously. The 1730 cm^{-1} peak, associated with the C=O bond, increases for OGV 1, 2 and 3 following ageing. It is slightly smaller for OGV 4 despite its long flight service time. The peak at 1650 cm^{-1} has increased for OGV 1 and 2. It could be associated with the increase in C=O bonds following oxidation (71; 72), but also to the increase in O–H bonds following the arrival of water molecules (56). The strongest

variation in peak intensity is noted for the series of peaks from 1225 to 850 cm^{-1}. They are most intense for OGV 2 and 3. As with the surface spectra, they could be related to the presence of contaminants or chemical evolution. This does not seem to be related to moisture since OGV 3 is also affected. OGV 4 seems less affected even though it has a long service life, perhaps because it has evolved in a less hostile climate.

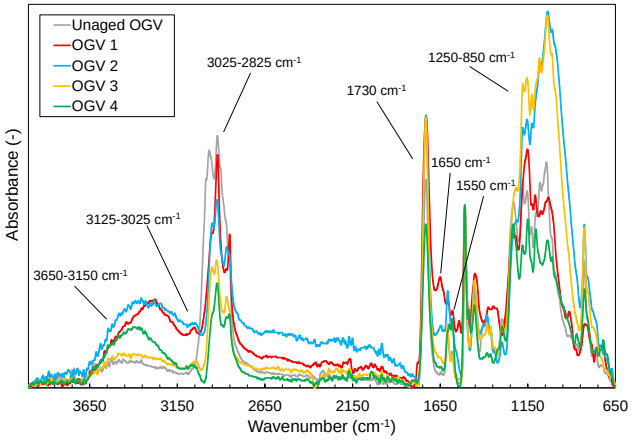

Figure 4. FTIR spectra of OGV foams.

Water content by Karl Fischer titration

Optimisation of Karl Fischer titrator parameters The Karl Fischer coulometric titrator has an autosampler with an oven to extract water. It is necessary to determine an analysis temperature above the glass transition temperature T_g and below the temperature at which the sample starts to degrade. The T_g of unaged OGV surfaces and foams are 179.5 ± 5.1 °C and 135.1 ± 0.4 °C, respectively. The degradation temperatures are 230.8 ± 0.8 °C and 218.8 ± 0.3 °C, respectively (obtained by Mettler TGA Star1).

The drift of unaged OGV surfaces is then analysed over a temperature range of 50 to 250 °C (Figure 5). This is the iodine amount generated per minute, correlated to the titrated water content. The drift analysis allows the identification of three distinct zones. A first break in slope is observed at 87.1 °C. It corresponds to the beginning of free water evaporation. A second break appears at 163.4 °C, a temperature close to the T_g, and can be associated with the beginning of the bound water release. It is, therefore, necessary to choose an extraction temperature lower than the degradation temperature and higher than 163.4 °C to allow the release of bound water. This is set at 180 °C. Different extraction methods may be used, depending on how the sample is handled. The implementation of three methods is detailed in the following.

Water content by standard Karl Fischer titration Standard Karl Fischer, titration by coulometry, is performed on samples of OGV 1 following the previous protocol. The measured water content is 0.25 ± 0.05 %.

Water content by Karl Fischer titration using chemical extraction Titration by chemical extraction consists of the total immersion of the solid sample in a solvent, in this case ethanol, in the hermetically sealed vial. The solvent will

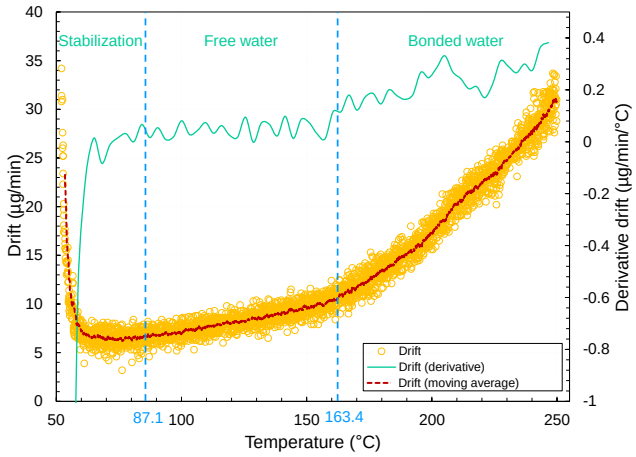

Figure 5. A drift of the unaged OGV FRP surface for a gradient of 50-250 °C, 1 °C/min.

allow the water in the composite to be extracted. During the oven passage, the water and ethanol are evaporated, but only the water reacts with the coulomat. Nevertheless, the ethanol used may contain a certain amount of water, which must be deduced from the measured content. For this purpose, five absolute ethanol analyses were used to validate a water content of 0.13 %. The following formula is used to determine the water content of the sample:

$$M_{water\ sample} = \frac{m_{water\ measured} - 0,0013 \times m_{ethanol}}{m_{sample}} \times 100 \quad (3)$$

with $M_{water\ sample}$ the water content of the sample (in %), $m_{water\ measured}$ the water mass measured in the sample, $m_{ethanol}$ the ethanol mass used in the test and m_{sample} the sample total mass before the test.

After titration by chemical extraction, the water measurement is more precise (Figure 6). Indeed, there is no stabilisation phase. When there is no preliminary extraction as before, more energy is needed to access the core water.

Figure 7 shows the water content evolution as a function of ethanol extraction time for OGV 1 FRP surface samples. After 3 days and 10 hours of immersion in ethanol, a stabilisation of the water content evolution is observed. The water that could be extracted by swelling with ethanol is extracted after 4 days and 15 hours. Beyond that, an instability of the drift shows that other phenomena disturb the measurement.

By the ethanol extraction method, we obtain a much closer water content equal to 0.68 ± 0.02 %. Chemical extraction with ethanol appears to be an efficient way to extract and measure more water from the sample.

Water content by Karl Fischer titration using grinding In the Karl Fischer titration by grinding, the sample is ground to a powder before passing through the Karl Fischer titrator. The average value obtained is 0.56 ± 0.03 % of water, which is lower than the results by chemical extraction.

Method comparison Finally, the three titration methods were used on samples from OGV 1 to compare their

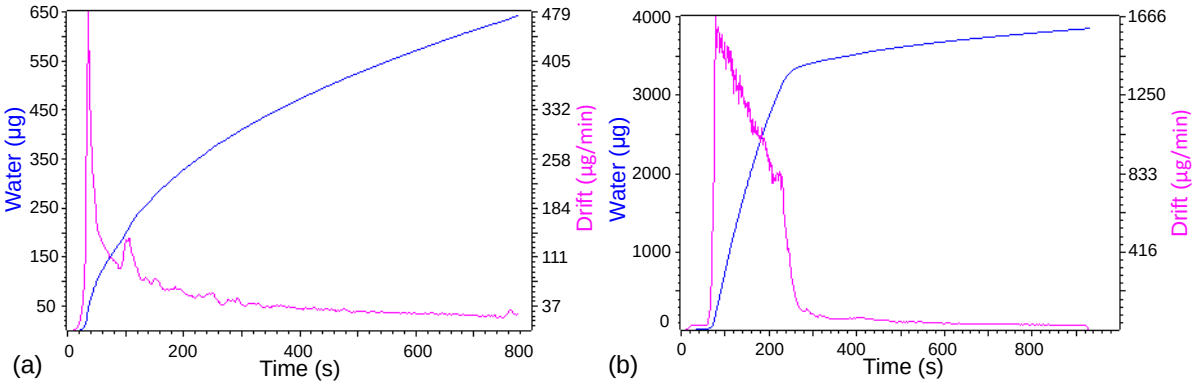

Figure 6. Karl Fischer analyses (a) standard (without chemical extraction), (b) with chemical extraction.

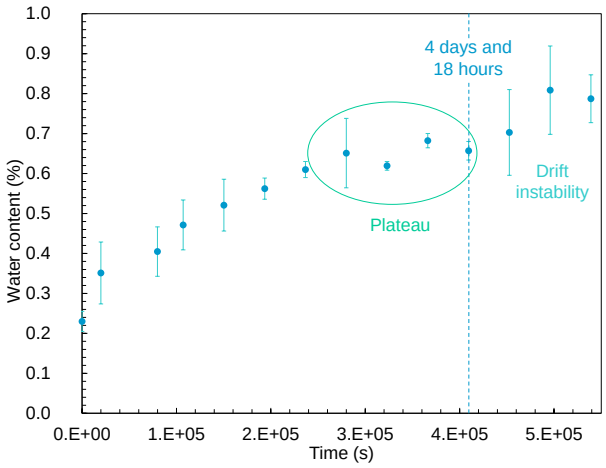

Figure 7. Water content evolution as a function of the time of chemical extraction with ethanol.

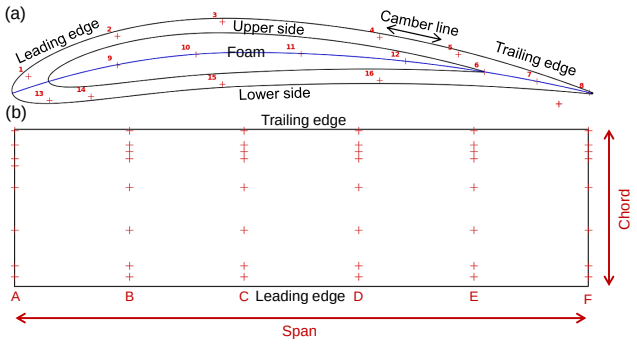

Figure 8. NACA airfoil, distribution of the 16 measuring points on a cross-section of the OGV blade: (a) Cross-section, (b) Top view.

results. Water contents measured by the different methods on samples from FRP surface OGV 1 are listed in Table 3.

In the Karl Fischer standard titration, the curve did not reach a plateau within the test time. The water may not be completely extracted. A plateau is more clearly visible on the curve by chemical extraction, although a slight slope is still observable. In addition, it could also be due to the moisture present in the air injected during the test. During sample grinding, heating and an increase in the exchange surface area may occur, allowing some free water to evaporate (73; 74).

Distribution of water content across the scrapped OGV

Mapping In order to represent the water content distribution across an OGV blade, a NACA 4-digit airfoil is used. 16 sampling points are determined to allow full coverage of a cross-section: 5 on the upper side, 4 on the lower side, 3 common to the upper and lower sides and 4 in the foam. A finer mesh size is not envisaged, as the measurement requires that the samples have the minimum masses indicated in the "Material and Methods" section (Figure 8). 6 cross-sections are then made along the blade, for a total of 96 sampling points per blade. The mapping of the OGV blade is carried out with the *Python* language and the *Spyder* software. The standard Karl Fischer titration method is chosen, despite a supposedly imperfect measurement, to measure concentration gradients in a short test time.

The first mapping is done on an OGV 2 blade. Figure 9 represents the 6 cross-sections, whereas Figure 10 shows the longitudinal sections, in the upper side, the foam and the lower side.

The water saturation is not reached. An inhomogeneous distribution of the water content is noticeable across the blade. The foam has accumulated less water (between 0.3 and 0.45 %) than the FRP surfaces (between 0.4 and 0.7 %). There is, therefore, a gradient in water concentration across the thickness. This difference in water content can be explained because the foam is not in direct contact with the outside environment. In addition, foam and FRP probably do not have the same absorption capacity, as shown by the significant differences in water content when going from the upper side to the foam or from the lower side to the foam. Furthermore, a large disparity in water content is observed along the chord of the OGV, both in the FRP (upper of lower side) and in the foam. In contrast, a certain homogeneity is observed along the span. Areas of high water concentration on the upper side correspond to areas of high water concentration in the foam. Diffusion in the thickness drives the water evolution within the part. Concerning the lower side, the two areas with higher concentrations are not associated with the foam. The upper side shows concentrations up to 1.5 to 2 times higher than the lower side at the leading edge, protected by the bonded stainless steel foil. The adhesive may have accelerated the water diffusion.

Table 3. Water content (in %) of FRP surface OGV 1 samples and testing time according to the method used.

Method	Water content (%)	Test time	T_{max} (°C)
Karl Fischer (standard)	0.25 ± 0.05	20 minutes	180
Karl Fischer (chemical extraction)	0.68 ± 0.02	4 days and 18 hours	180
Karl Fischer (grinding)	0.56 ± 0.03	20 minutes	180

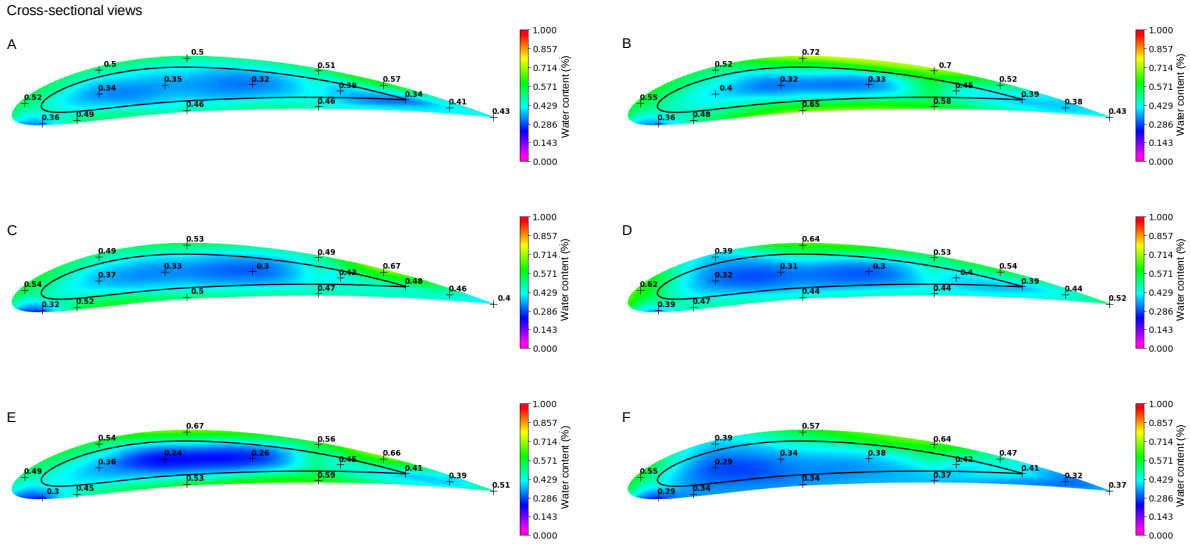

Figure 9. Water contents in the 6 cross-sections of an OGV 2 blade.

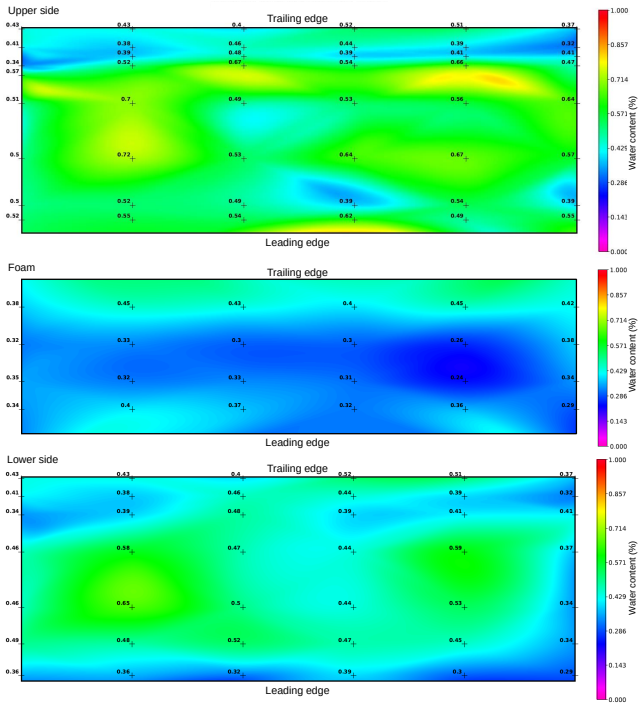

Figure 10. Water contents along the longitudinal sections of an OGV 2 blade (upperside, foam and lower side).

The same mappings are achieved for OGV 3 blade (Figure 11) and OGV 4 blade (Figure 12).

The highest water contents are observed on the FRP surfaces, mainly the lower side, of the OGV 3. The water contents within the foam are the lowest. Diffusion through the material seems less advanced. A high degree of heterogeneity is observed along the span, with sections E and F showing significant water content. Abnormal water diffusion may have occurred through the upper platform adhesive, which is sensitive to moisture uptake.

OGV 4 has an intermediate water content, with, as with OGV 3, a more affected lower side. In all three cases, a water gradient is located at the leading edge, covered with the bond stainless steel foil. Moisture diffusion seems to take place around this area.

The water content measurements made on OGV 2, 3 and 4 by Karl Fischer standard titration are summarised in Table 4. According to the three results, OGV 2, which flew in hot and humid climates, shows the lowest water contents by titration.

Discussion

The microscopic observations highlight differences between the upper and lower sides (Figure 2). Damage is more intense on the lower side than on the upper side. This difference could be due to the pressure and velocity differences along the OGV NACA airfoil (75; 76; 77; 78). On the OGVs in this paper, the carbon fibres, cracked in some areas, are exposed. Although they are susceptible to be more in contact with water, these more attacked areas also contain the lowest water content. They also correspond to the areas with greater air flow and, therefore, higher pressures and temperatures.

Two hypotheses can be made. The lower water content observed in these areas could suggest that the turbulent air flow at high temperature and high pressure during flight would have a drying effect greater than the moisture-absorbing effect of the material. However, these observations do not coincide with the water contents of OGV 3 and 4. The other hypothesis is that the air flow, and particles and water drops it carries away have an abrasive effect on the OGV surfaces. Several authors have demonstrated the erosive effect of dust and pollution particles or water drops sent at high speed on composite materials (79; 80; 81; 82).

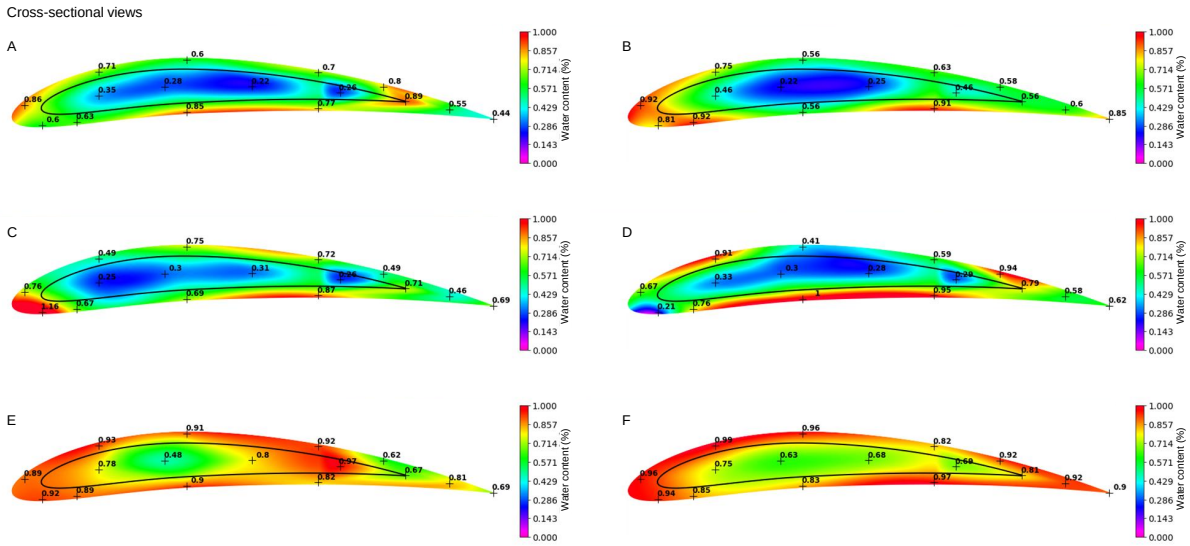

Figure 11. Water contents in the 6 cross-sections of an OGV 3 blade.

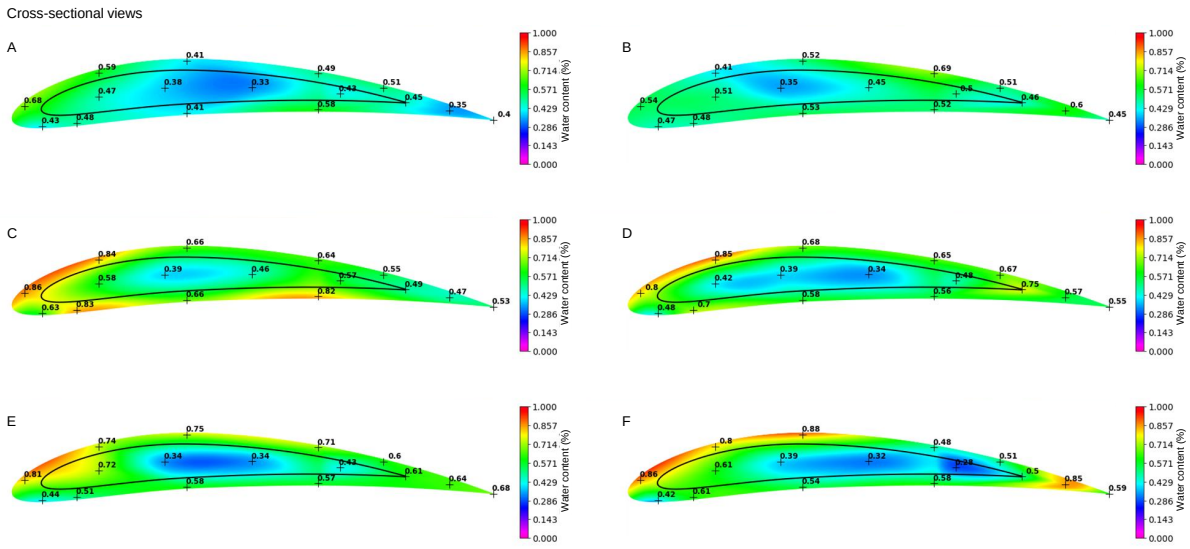

Figure 12. Water contents in the 6 cross-sections of an OGV 4 blade.

Table 4. Water content (in %) of OGV 2, 3 and 4 (Karl Fischer standard titration).

Name	FRP surface (titration)	Foam (titration)
OGV 2	$0.29 - 0.72$	$0.24 - 0.45$
OGV 3	$0.21 - 1.16$	$0.22 - 0.97$
OGV 4	$0.35 - 0.88$	$0.28 - 0.72$

The OGV 2 matrices, which are more brittle due to the hot and humid ageing in which they evolve, as stipulated by the drop in T_g and the microscopic observations, could be eroded more easily by this turbulent and hot air flow. Indeed, they have been subjected to chain scissions by hydrolysis or oxidation during ageing, as observed on the FTIR spectra. The crack propagation already present on the surface can be accelerated by thermo-oxidation (83). The resin content on the surface would then be strongly reduced, which could also impact the water content measurement. Indeed, comparing the upper sides to the lower sides of the OGV 2 in Figure 10, it appears that the upper sides, less damaged, coincide with areas with higher water content shown on Figure 9. When comparing with OGV 3 and 4, it can be seen that they have experienced less erosion than the OGV 2 blades. They may have lost less resin, which could explain their higher water content than OGV 2.

Additional data could have supported the study. Depending on the placement of the OGV on the engine crown, the ambient humidity is susceptible to change. The parts located at 6 o'clock on the crown, i.e. those furthest south, are subject to the gravity fall of water drops and their stagnation. Therefore, these parts may have been in repeated contact with water due to their position in the engine. Furthermore,

several authors have shown that, depending on the blades' angle of attack and their shape, the contours of static pressure and the contours of velocity magnitude around the NACA airfoil evolve (84; 85). Depending on its position and angle, these pressure differences along the blade should impact the air flows and damage caused.

Conclusion

In this paper, different methods of water content measurement by Karl Fischer titration are used and compared. These methods show advantages and disadvantages. The standard coulometric Karl Fischer titration method provides results in a short test time (about 20 min) and thus allows the treatment of a large sample number in an automated and fast way. However, this method does not seem to be able to remove all the water from samples of composite materials. It is possible that some bound water still remains, which requires a higher temperature to be released, with a degradation risk for the samples. Nevertheless, it is possible with this method to determine the presence of water concentration gradients within a part. The grinding method allows more water to be removed than the standard method in the same amount of time. However, it may be inaccurate due to the heating that grinding the sample produces. A volumetric rather than coulometric titration could have addressed this water loss problem. The chemical extraction method is the Karl Fischer titration method used in this paper, which provides the highest water contents. It could be closest to reality without introducing heating and thermal degradation to the sample. On the other hand, the test is much longer, almost 5 days. It is, therefore, unappropriate to quickly process a large number of samples, like in this test campaign of 96 samples per blade.

The standard Karl Fischer titration was used on 3 Outlet Guide Vanes blades to determine variations in water content and water gradient concerning the climate of the OGV flight service life areas. Although the water content measurement is not complete, the OGV in the study can be compared with each other, and concentration gradients appear along the blades. No OGV reached water saturation. Various observations were made, including that the water contents of OGV 2, which operated in a hot and humid climate, were the lowest, with water contents between 0.29 and 0.75 $\%$ for the FRP surface. Because of these results and in a context of natural ageing where many phenomena are coupled, combining these water content measurements with other characterisation tests is necessary. The observation of significant matrix erosion, fibre exposure and cracking on the surface, and the drop in T_g by around 23.5 °C, confirms that OGV 2 has suffered the most degradation. Environmental effects, heat peaks and air flows more easily eroded the weakened resin. The lack of resin could therefore explain these low water content measurements. It would then be interesting to couple the mapping obtained by Karl Fisher titration to a fluid mechanics analysis for this type of OGV and aircraft engine.

Acknowledgements

The authors express their sincere thanks to SAFRAN Aircraft Engines, France, and the Association Nationale de la Recherche et de la Technologie for the financial support (ANRT CIFRE n°2018/0355 project). They are grateful to Amandine Abadie at the Laboratoire Génie de Production (France), and to Blandine Batschelet at Safran Aircraft Engines (France), for their technical support.

References

References

[1] Peters, S.& Hadcock, R. N. Aircraft applications. *Handbook Of Composites*. pp. 1022-1044 (1998)

[2] Vodicka, R., Nelson, B., Berg, J. & Chester, R. Long-term environmental durability of F/A-18 composite material. (DSTO Aeronautical,1999)

[3] Stone, R. Flight service evaluation of advanced composite ailerons on the L-1011 transport aircraft. (NASA,1987)

[4] Billy, F. Vieillissement et propriétés résiduelles de matériaux issus du démantèlement d'avions en fin de vie. (École nationale supérieure de mécanique et d'aérotechnique,2013)

[5] Dexter, H. & Baker, D. Flight service environmental effects on composite materials and structures. *Advanced Performance Materials*. **1**, 51-85 (1994)

[6] Tian, W. & Hodgkin, J. Long-term aging in a commercial aerospace composite sample: Chemical and physical changes. *Journal Of Applied Polymer Science*. **115**, 2981-2985 (2010)

[7] McKague, E., Halkias, J. & Reynolds, J. Moisture in composites: the effect of supersonic service on diffusion. *Journal Of Composite Materials*. **9**, 2-9 (1975)

[8] Collings, T. & Stone, D. Hygrothermal effects in CFC laminates: Damaging effects of temperature, moisture and thermal spiking. *Composite Structures*. **3**, 341-378 (1985)

[9] Tsotsis, T. Considerations of failure mechanisms in polymer matrix composites in the design of aerospace structures. *Failure Mechanisms In Polymer Matrix Composites*. pp. 227-278 (2012)

[10] Jonsson, I., Deshpande, S., Chernoray, V., Thulin, O. & Larsson, J. Experimental and Numerical Study of Laminar-Turbulent Transition on a Low-Pressure Turbine Outlet Guide Vane. *Turbo Expo: Power For Land, Sea, And Air*. **84072** pp. V02BT33A014 (2020)

[11] Wang, C., Wang, L., Sundén, B., Chernoray, V. & Abrahamsson, H. An experimental study of heat transfer on an outlet guide vane. *Turbo Expo: Power For Land, Sea, And Air*. **45721** pp. V05BT14A001 (2014)

[12] Voronkov, A., Kosheleva, N. & Pelenev, K. Experimental Study of the Stress-Strain State Features of Outlet Guide Vane Made From Polymer Composite Material Using Fiber Optic Sensors. *2018 International Multi-Conference On Industrial Engineering And Modern Technologies (FarEastCon)*. pp. 1-5 (2018)

[13] Kaminski-Morrow, D. Corrosion crack led Korean 777-300's axle to snap. *Flight Global*. (2019)

[14] Chong, A. Turbine blade corrosion caused Jet ATR engine fire. *Flight Global*. (2018)

[15] Sugita, Y., Le, P. & Saponara, V. Effect of jet fuel, hydraulic fluid, water on performance of carbon/epoxy lap-joints. (2007)

[16] Sala, G. Composite degradation due to fluid absorption. *Composites Part B: Engineering*. **31**, 357-373 (2000)

[17] Peters, S., Whitaker, A. F., Finckenor, M., Dursch, H., Tennyson, R. & Young, P. R. Environmental effect on composites. *Handbook Of Composites*. pp. 810-821 (1998)

[18] White, J. & Turnbull, A. Weathering of polymers: mechanisms of degradation and stabilization, testing strategies and modelling. *Journal Of Materials Science*. **29**, 584-613 (1994)

[19] Funke, W. & Haagen, H. Influence of sulfur dioxide on organic coatings. (ACS Publications,1983)

[20] Jakubowicz, I. & Möller, K. An FTIR, impact strength and thermal analysis investigation of a PVC window frame naturally aged for 20 years. *Polymer Degradation And Stability*. **36**, 111-120 (1992)

[21] Colin, X., Richaud, E. & Monchy-Leroy, C. Couplages dans le vieillissement des matériaux organiques. *Matériaux & Techniques*. **97** pp. 325-337 (2009)

[22] Simar, A. Impact du vieillissement humide sur le comportement d'un composite à matrice organique tissé fabriqué par injection RTM: Mise en évidence d'un couplage entre absorption d'eau et thermo-oxydation de la matrice. (École nationale supérieure de mécanique et d'aérotechnique,2014)

[23] Tchalla, T. Durabilité d'assemblages métal/élastomère en milieu marin. (Université Bretagne-Loire,2017)

[24] Colin, X. & Verdu, J. Humid Ageing of Organic Matrix Composites. *Durability Of Composites In A Marine Environment*. pp. 47-114 (2014)

[25] Adamson, M. Thermal expansion and swelling of cured epoxy resin used in graphite/epoxy composite materials. *Journal Of Materials Science*. **15**, 1736-1745 (1980)

[26] Colin, X., Verdu, J. & Rabaud, B. Stabilizer Thickness Profiles in Polyethylene Pipes Transporting Drinking Water Disinfected by Bleach. *Polymer Engineering And Science*. **51**, 1539-1549 (2011)

[27] Xiao, G. & Shanahan, M. Swelling of DGEBA/DDA epoxy resin during hygrothermal ageing. *Polymer*. **39**, 3253-3260 (1998)

[28] Tcharkhtchi, A., Bronnec, P. & Verdu, J. Water absorption characteristics of diglycidylether of butane diol–3,5-diethyl-2,4-diaminotoluene networks. *Polymer*. **41**, 5777-5785 (2000)

[29] Weitsman, Y. Anomalous fluid sorption in polymeric composites and its relation to fluid-induced damage. *Composites Part A: Applied Science And Manufacturing*. **37**, 617-623 (2006)

[30] Popineau, S., Rondeau-Mouro, C., Sulpice-Gaillet, C. & Shanahan, M. Free/bound water absorption in an epoxy adhesive. *Polymer*. **46**, 10733-10740 (2005)

[31] Dao, B., Hodgkin, J., Krstina, J., Mardel, J. & Tian, W. Accelerated aging versus realistic aging in aerospace composite materials. V. The effects of hot/wet aging in a structural epoxy composite. *Journal Of Applied Polymer Science*. **115**, 901-910 (2010)

[32] De'Nève, B. & Shanahan, M. Water absorption by an epoxy resin and its effect on the mechanical properties and infra-red spectra. *Polymer*. **34**, 5099-5105 (1993)

[33] Simar, A., Gigliotti, M., Grandidier, J. & Ammar-Khodja, I. Decoupling of water and oxygen diffusion phenomena in order to prove the occurrence of thermo-oxidation during hygrothermal aging of thermosetting resins for RTM composite applications. *Journal Of Materials Science*. **53**, 11855-11872 (2018)

[34] Bonniau, P. & Bunsell, A. A comparative study of water absorption theories applied to glass epoxy composites. *Journal Of Composite Materials*. **15**, 272-293 (1981)

[35] Alston, S., Korkees, F. & Arnold, C. Finite element modelling of moisture uptake in carbone fibre/epoxy composites : a multi-scale approach. *ECCM15 Proceedings*. (2012)

[36] Zhou, J. & Lucas, J. The effects of a water environment on anomalous absorption behavior in graphite/epoxy composites. *Composites Science And Technology*. **53**, 57-64 (1995)

[37] Xiao, G. & Shanahan, M. Irreversible effects of hygrothermal aging on DGEBA/DDA epoxy resin. *Journal Of Applied Polymer Science*. **69**, 363-369 (1998)

[38] Abdessalem, A., Tamboura, S., Fitoussi, J., Ben Daly, H. & Tcharkhtchi, A. Bi-phasic water diffusion in sheet molding compound composite. *Journal Of Applied Polymer Science*. **137**, 1-12 (2020)

[39] Deroiné, M., Le Duigou, A., Corre, Y., Le Gac, P., Davies, P., César, G. & Bruzaud, S. Accelerated ageing of polylactide in aqueous environments: Comparative study between distilled water and seawater. *Polymer Degradation And Stability*. **108** pp. 319-329 (2014)

[40] Berthé, V., Ferry, L., Bénézet, J. & Bergeret, A. Ageing of different biodegradable polyesters blends mechanical and hygrothermal behavior. *Polymer Degradation And Stability*. **95**, 262-269 (2010)

[41] El Yagoubi, J., Lubineau, G., Roger, F. & Verdu, J. A fully coupled diffusion-reaction scheme for moisture sorption–desorption in an anhydride-cured epoxy resin. *Polymer*. **53**, 5582-5595 (2012)

[42] Gillet, C., Nassiet, V., Poncin-Epaillard, F., Hassoune-Rhabbour, B. & Tchalla, T. Chemical Behavior of Water Absorption in a Carbon/Epoxy 3D Woven Composite. *Macromolecular Symposia*. **405**, 2100213 (2022)

[43] Gillet, C., Hassoune-Rhabbour, B., Poncin-Epaillard, F., Tchalla, T. & Nassiet, V. Contributions of atmospheric plasma treatment on a hygrothermal aged carbon/epoxy 3D woven composite material. *Polymer Degradation And Stability*. **202** pp. 110023 (2022)

[44] Gillet, C., Tamssaouet, F., Hassoune-Rhabbour, B., Tchalla, T. & Nassiet, V. Parameters Influencing Moisture Diffusion in Epoxy-Based Materials during Hygrothermal Ageing—A Review by Statistical Analysis. *Polymers*. **14**, 2832 (2022)

[45] Ouled Ahmed, R., Chatti, S. & Ben Daly, H. Modeling of hygrothermal damage of composite materials. *Mechanics Of Advanced Composite Structures*. **3**, 137-144 (2016)

[46] El Yagoubi, J., Lubineau, G., Traidia, A. & Verdu, J. Monitoring and simulations of hydrolysis in epoxy matrix composites during hygrothermal aging. *Composites Part A: Applied Science And Manufacturing*. **68** pp. 184-192 (2015)

[47] Weitsman, Y. & Guo, Y. A correlation between fluid-induced damage and anomalous fluid sorption in polymeric composites. *Composites Science And Technology*. **62**, 889-908 (2002)

[48] Guo, F., Huang, P., Li, Y., Hu, N. & Fu, S. Multiscale modeling of mechanical behaviors of carbon fiber reinforced epoxy composites subjected to hygrothermal aging. *Composite Structures*. **256** pp. 113098 (2021)

[49] Zhou, J. & Lucas, J. Hygrothermal effects of epoxy resin. Part I: the nature of water in epoxy. *Polymer*. **40**, 5505-5512 (1999)

[50] Grangeat, R., Girard, M., Lupi, C., Leduc, D. & Jacquemin, F. Measurement of the local water content of an epoxy adhesive by fiber optic sensor based on Fresnel reflection. *Mechanical Systems And Signal Processing*. **141** pp. 106439 (2020)

[51] Grangeat, R., Girard, M., Lupi, C. & Jacquemin, F. Local water content field within an epoxy/metal bonded assembly in immersion. *The Journal Of Adhesion*. pp. 1-17 (2022)

[52] Mieloszyk, M. & Ostachowicz, W. Moisture contamination detection in adhesive bond using embedded FBG sensors. *Mechanical Systems And Signal Processing*. **84** pp. 1-14 (2017)

[53] Mieloszyk, M., Majewska, K. & Ostachowicz, W. THz spectroscopy application for detection and localisation of water inclusion in glass composite. *Composite Structures*. **192** pp. 537-544 (2018)

[54] Krauklis, A., Gagani, A. & Echtermeyer, A. Near-infrared spectroscopic method for monitoring water content in epoxy resins and fiber-reinforced composites. *Materials*. **11**, 586 (2018)

[55] Idolor, O., Guha, R., Berkowitz, K., Geiger, C., Davenport, M. & Grace, L. Polymer-water interactions and damage detection in polymer matrix composites. *Composites Part B: Engineering*. **211** pp. 108637 (2021)

[56] Musto, P., Ragosta, G. & Mascia, L. Vibrational spectroscopy evidence for the dual nature of water sorbed into epoxy resins. *Chemistry Of Materials*. **12**, 1331-1341 (2000)

[57] Larsson, W., Jalbert, J., Gilbert, R. & Cedergren, A. Efficiency of methods for Karl Fischer determination of water in oils based on oven evaporation and azeotropic distillation. *Analytical Chemistry*. **75**, 1227-1232 (2003)

[58] De Caro, C., Aichert, A. & Walter, C. Efficient, precise and fast water determination by the Karl Fischer titration. *Food Control*. **12**, 431-436 (2001)

[59] Kestens, V., Conneely, P. & Bernreuther, A. Vaporisation coulometric Karl Fischer titration: A perfect tool for water content determination of difficult matrix reference materials. *Food Chemistry*. **106**, 1454-1459 (2008)

[60] Shi, Y., Tay, A., Wong, E. & Ranjan, R. An effective method of characterizing moisture desorption of polymeric materials at high temperature. *4th Electronics Packaging Technology Conference, 2002.*. pp. 70-75 (2002)

[61] He, N. & Lindfors, T. Determination of water uptake of polymeric ion-selective membranes with the coulometric Karl Fischer and FT-IR-attenuated total reflection techniques. *Analytical Chemistry*. **85**, 1006-1012 (2013)

[62] Ranaweera, R., Schuman, T., Wang, R., Miller, B. & Kilway, K. Effect of moisture on cationic polymerization of silicone epoxy monomers. *Journal Of Applied Polymer Science*. **132** (2015)

[63] Lin, Y., Chen, X., Zhang, H. & Wang, Z. Effects of hygrothermal aging on epoxy-based anisotropic conductive film. *Materials Letters*. **60**, 2958-2963 (2006)

[64] Cherdoud-Chihani, A., Mouzali, M. & Abadie, M. Study of crosslinking AMS/DGEBA system by FTIR. *Journal Of Applied Polymer Science*. **69**, 1167-1178 (1998)

[65] González, M., Cabanelas, J. & Baselga, J. Applications of FTIR on epoxy resins-identification, monitoring the curing process, phase separation and water uptake. *Infrared Spectroscopy-Materials Science, Engineering And Technology*. pp. 261-284 (2012)

[66] Scholz, E. Karl Fischer titration: determination of water. (Springer Science & Business Media,2012)

[67] Pretsch, E., Bühlmann, P., Affolter, C., Pretsch, E., Bhuhlmann, P. & Affolter, C. Structure determination of organic compounds. (Springer,2000)

[68] Nakanishi, K., Solomon, P. & Others Infrared absorption spectroscopy. (Holden-day,1977)

[69] Bellamy, L. The infra-red spectra of complex molecules. (Springer Science & Business Media,2013)

[70] Dao, B., Hodgkin, J., Krstina, J., Mardel, J. & Tian, W. Accelerated aging versus realistic aging in aerospace composite materials. II. Chemistry of thermal aging in a structural composite. *Journal Of Applied Polymer Science*. **102**, 3221-3232 (2006)

[71] Pei, Y., Wang, K., Zhan, M., Xu, W. & Ding, X. Thermal-oxidative aging of DGEBA/EPN/LMPA epoxy system: chemical structure and thermal–mechanical properties. *Polymer Degradation And Stability*. **96**, 1179-1186 (2011)

[72] Krauklis, A. & Echtermeyer, A. Mechanism of Yellowing: Carbonyl Formation during Hygrothermal Aging in a Common Amine Epoxy. *Polymers*. **10**, 1-15 (2018)

[73] Sasahara, H., Kikuma, T., Koyasu, R. & Yao, Y. Surface grinding of carbon fiber reinforced plastic (CFRP) with an internal coolant supplied through grinding wheel. *Precision Engineering*. **38**, 775-782 (2014)

[74] Khoran, M., Azarhoushang, B. & Amirabadi, H. Evaluating the influence of reinforcing fiber type on the grinding process of PEEK's composites. *The International Journal Of Advanced Manufacturing Technology*. pp. 1-14 (2022)

[75] Ben Nasr, N. & Gerolymos, G. RSM RANS Computation of Aircraft Engine Fan/OGV Unsteady Aerodynamics for Noise-Prediction Input. *15th AIAA/CEAS Aeroacoustics Conference (30th AIAA Aeroacoustics Conference)*. pp. 3151 (2009)

[76] Polacsek, C., Daroukh, M., François, B. & Barrier, R. Turbofan broadband noise predictions based on a ZDES calculation of a fan-OGV stage. *Forum Acusticum 2020*. (2020)

[77] Walker, A., Barker, A., Carrotte, J., Bolger, J. & Green, M. Integrated outlet guide vane design for an aggressive S-shaped compressor transition duct. *Journal Of Turbomachinery*. **135**, 011035 (2013)

[78] Lewis, D. From analytical to fully numerical predictions of the broadband noise radiated by a full fan-OGV stage. (École Centrale de Lyon,2020)

[79] Drensky, G., Hamed, A., Tabakoff, W. & Abot, J. Experimental investigation of polymer matrix reinforced composite erosion characteristics. *Wear*. **270**, 146-151 (2011)

[80] Groucott, S., Pugh, K., Zekos, I. & M Stack, M. A study of raindrop impacts on a wind turbine material: velocity and impact angle effects on erosion MAPS at various exposure times. *Lubricants*. **9**, 60 (2021)

[81] Tewari, U., Harsha, A., Häger, A. & Friedrich, K. Solid particle erosion of carbon fibre–and glass fibre–epoxy composites. *Composites Science And Technology*. **63**, 549-557 (2003)

[82] Zahavi, J., Nadiv, S. & Schmitt Jr, G. Indirect damage in composite materials due to raindrop impact. *Wear*. **72**, 305-313 (1981)

[83] Colin, X., Mavel, A., Marais, C. & Verdu, J. Interaction between cracking and oxidation in organic matrix composites. *Journal Of Composite Materials*. **39**, 1371-1389 (2005)

[84] Singh, J., Singh, J., Singh, A., Rana, A. & Dahiya, A. Study of NACA 4412 and Selig 1223 airfoils through computational fluid dynamics. *SSRG International Journal Of Mechanical Engineering (SSRG-IJME)–volume*. **2**, 17-21 (2015)

[85] Rubel, R., Uddin, M., Islam, M. & Rokunuzzaman, M. Numerical and experimental investigation of aerodynamics characteristics of NACA 0015 aerofoil. *International Journal Of Engineering Technologies IJET*. **2**, 132-141 (2016)